



ELSEVIER

Contents lists available at ScienceDirect

## Journal of Magnetism and Magnetic Materials

journal homepage: [www.elsevier.com/locate/jmmm](http://www.elsevier.com/locate/jmmm)

## Research articles

## The development of a micro-coil-on-ASIC type GSR sensor driven by GHz pulse current

Yoshinobu Honkura<sup>a</sup>, Shinpei Honkura<sup>b</sup><sup>a</sup> *Magnedesign Corporation, Nagoya, Japan*<sup>b</sup> *Nanocoil Corporation, Nagoya, Japan*

## ARTICLE INFO

## Keywords:

GSR sensor  
GMI sensor  
Amorphous micro wire  
GHz Pulse current

## ABSTRACT

Through applying GHz (Gigahertz) pulse current on the amorphous micro wire, we observed an increase in the coil voltage around the wire, and a sine function relationship between the coil voltage and the surrounding magnetic field. We assumed that the new performance of the coil voltage must be caused by the rotation of electron spins on the wire surface with GHz angular velocity, induced by the magnetic field force in the same direction, and proposed to name the observed new phenomena as GSR (Gigahertz Spin Rotation) effect. The developed GSR sensor presents excellent features with enhanced sensitivity and low hysteresis better than that of the GMI (Giant Magnetoimpedance) sensor.

We developed the production technology to produce micro coils and developed a Micro-coil-on-ASIC (Application Specified Integrated Circuit) type GSR sensor, where the micro coils are directly formed on the ASIC surface, making small size GSR sensor possible.

## 1. Introduction

The magnetic sensors which make up about 30% of the sensors market [1–4] plays a relevant role in industries related to sensorics, like automotive use, medical use, consumers and so on.

Small sized and highly sensitive magnetic sensors have been developed for the innovation of magnetic sensor systems. They are mainly classified into three kinds of magnetic sensors. The first one is the coil type magnetic sensor such as FG (Flux Gate) sensor, coil type GMI sensor and GSR sensor, which detect the magnetization change in the magnetic core material as the coil voltage. The second type is the magnetic resistance type such as MR (Magneto resistance), AMR (anisotropic magnetoresistance), GMR (Giant Magnetoresistance), TMR (Tunnel effect Magnetoresistance) and GMI, which detect the change of magnetic resistance or magnetic impedance. Third type is Hall sensor which detects the hall voltage.

Various kinds of magnetic materials are used for coil type magnetic sensors, i.e., Iron, Si-steel, Permalloy Soft ferrite, amorphous alloy and so on. The amorphous magnetic wire developed by Prof. Ohnaka and Prof. Masumoto [5,6] in Japan has high permeability and high resistance. Its magnetic domain structure was studied by Prof. Yamazaki and Prof. Humphrey [7,8]. In 1987 using the amorphous wire, a magnetic sensor driven by pulse current was developed TDK Corporation [9] which had the frequency of 1 MHz, higher than the 50KHz of

conventional type FG sensor. Conventional type FG sensor effect is based on the magnetization rotation of the whole wire.

In 1991, GMI effect in amorphous materials under the frequency of 2 MHz was found by Prof. Makhotokin [10]. In 1993, Prof. Mohri developed the GMI sensor based on the GMI effect of the amorphous wire with a diameter of 30  $\mu\text{m}$ , which provided high sensitivity at the frequency of 10 MHz based on the skin effect [11–13]. The strong skin effect based on the GMI effect is caused by the high circumferential permeability of the surface domain shell in the wire [14–17].

In 1999, Prof. Mohri invented a coil type GMI sensor with a pulse frequency of 20 MHz [18–20]. This type of sensor has a linear output voltage against the external magnetic field. In 2004, Prof. Pania reported the principle of the coil type GMI sensor which conveyed that the off-diagonal impedance in amorphous wires made linear output against the external magnetic field [21]. In 2008, a small size coil type GMI was developed by Aichi Steel corporation [22] which consisted of amorphous wire with a diameter of 10  $\mu\text{m}$ , pulse frequency of 200 MHz and the circuit of ASIC type. This small size coil type GMI sensor has been used in electronic compasses for smartphones [23]. The coil type GMI sensor, developed by Professor Uchiyama in 2011 with improved signal to noise ratio, allows the detection of pT magnetic field generated by the biological objects [24]. In 2014, Prof. Zhukov studied the effect of high frequency on the GMI and off-diagonal GMI and reported that the GMI effect has a maximum output of about 200 MHz and decreases

E-mail addresses: [mdc\\_honkura@magnedesign.co.jp](mailto:mdc_honkura@magnedesign.co.jp) (Y. Honkura), [shinpei.honkura@nanocoil.co.jp](mailto:shinpei.honkura@nanocoil.co.jp) (S. Honkura).

<https://doi.org/10.1016/j.jmmm.2020.167240>

Received 2 December 2019; Received in revised form 5 July 2020; Accepted 14 July 2020

Available online 25 July 2020

0304-8853/ © 2020 Elsevier B.V. All rights reserved.

beyond 200 MHz [25]. However the frequency dependency of the off diagonal GMI effect is not reported.

In 2015 the authors studied the effect of GHz pulse on the coil voltage of the coil type GMI sensor and observed that its coil voltage had a maximum of 2 GHz. In the 7th IWMW held in Spain the same year [26], the authors reported that the sensitivity increases with an increase in the pulse frequency of up to 2 GHz. This result is different from the behavior of the GMI effect which showed the maximum sensitivity at a frequency of 200 MHz [27–29]. The authors also observed a sine functional relationship between the output voltage and the magnetic field. The sine functionality is proven by inverse transformation, which allows the converted data versus the magnetic field to achieve a very good linearity. The authors thought the sine functionality was caused by the magnetization rotation brought by the spin rotation with GHz angular velocity in the surface magnetic domain driven by the GHz pulse current, and named the new phenomena showing the sine functionality as GSR effect.

GSR effect is explained as follows. The wire has a surface domain with circular magnetization orientation. When external magnetic field is applied to the wire along the axis direction, the spins tilt toward the axis direction. The GHz pulse current flowing through the wire produces a strong circular magnetic field [30] and makes the spin rotate with GHz angular velocity, which is accompanied by magnetization rotation. The pickup coil detects the change in magnetization rotation through the coil voltage.

When the coil detects the magnetization rotation brought by spin rotation in the surface domain with circular spins, the theory states that the coil voltage increases proportionally to  $\sqrt{f}$  and the coil voltage dependent on the external magnetic field takes a sine functional relationship. The coil voltage may be proportional to the longitudinal magnetization of tilted spins ( $= M \sin\theta$ ) and the changing velocity of the longitudinal magnetization of tilted spins ( $2\pi f \cos\theta$ ), therefore, it may be proportional to  $2\pi f M \sin\theta$ . The theoretical expectation of  $2\pi f M \sin\theta$  is coincident to the experimental result. However when the frequency is over 3 GHz, the coil voltage decreases most likely because of ferromagnetic resonance. It must be noted that the magnetic domain walls cannot move because of the strong skin effect at GHz current pulse (the penetration skin depth at these frequencies is quite low below 1  $\mu\text{m}$ ) [31,32].

In this paper the research on the GSR effect carried out using the ASIC circuit and various type GSR Sensor elements, the production technology to produce micro coils directly on the ASIC surface and prototypes of GSR sensors for some promising applications are reported [33–36].

## 2. Research on the GSR effect

### 2.1. Principle of the GSR effect

The principle of the GSR effect induced in the amorphous wire with zero magnetostriction is explained using Fig. 1. The used Co-rich wire has a special magnetic domain structure which consists of surface domains with circular magnetization orientation, axially magnetized magnetic domains and 90 degree domain wall existing between two domains. When external magnetic field is applied to the wire along the

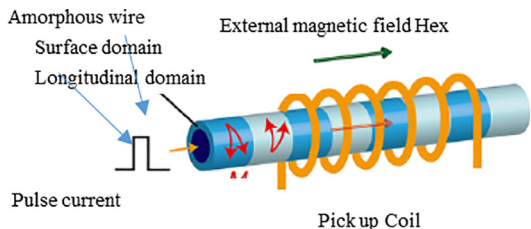


Fig. 1. Principle of GSR Effect.

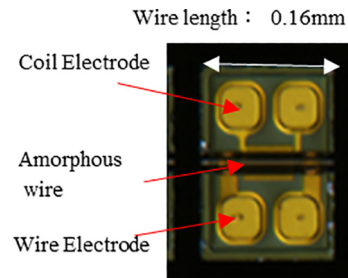


Fig. 2. Structure of GSR Element.

axis direction, electronic spins in surface domains tilt toward the axial direction with the angle dependent on the magnetic field strength. The inner magnetic domains present axial magnetization direction. The GHz pulse current that passes through the wire produces a strong circular magnetic field [30] and creates magnetization rotation brought by only spin rotation with GHz angular velocity that does not affect the inner domain (does not produce the domain wall movement) because of the strong skin effect induced by GHz current pulse.

Fig. 2 shows the typical structure of the GSR element, containing one glass coated amorphous wire, 2 wire electrodes and 2 coil electrodes with length of 0.16 mm and width of 0.23 mm. Fig. 3 shows an observed result of the wire voltage and the coil voltage induced by GHz pulse current. Here the applied pulse has a rising time or falling time of 0.5nsec and the pulse duration of 10nsec under the pulse repetition of 1 MHz. The peak coil voltage is indicated by the sharp edges of rising and falling of the wire pulse current. From this, the following things are predicted. 1) The GSR effect might increase the coil voltage with the increase in the frequency of GHz pulse current and coil turn numbers. 2) The magnetization rotation brought by spin rotation not accompanied by domain wall movements could improve magnetic properties of magnetic noise, hysteresis and linearity as well as sensitivity.

### 2.2. Experimental procedure

The present GSR element shown in Fig. 2 equips a wire with a composition of Co50.7Fe8.1B13.3Si10.3 and a relative permeability of 1800 with a diameter of 10  $\mu\text{m}$ . The tested GSR elements have lengths of 0.16 mm, 0.45 mm and 0.96 mm, wire resistance of 3  $\Omega$ , 8  $\Omega$ , 4.5  $\Omega$  and 13  $\Omega$ , coil turn numbers of 14, 32, 66 and 148 and coil resistance of 80  $\Omega$ , 210  $\Omega$ , 360  $\Omega$  and 810  $\Omega$  respectively.

The Block diagram and ASIC of the electronic circuit for the GSR sensor in Fig. 4(a) is similar to a conventional GMI circuit, but the ASIC used in this research has improvements as follows. The pulse generator

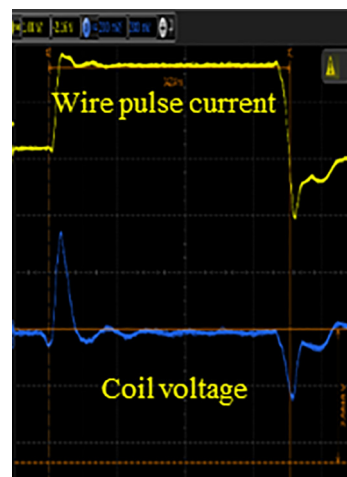


Fig. 3. Observed Coil Voltage.

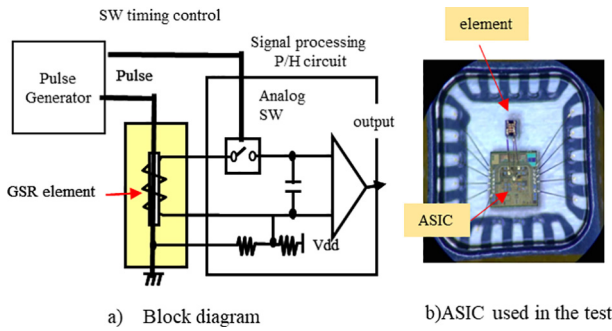


Fig. 4. The Circuit of GSR Sensor.

can generate pulse currents with frequencies from 1 GHz to 3 GHz. An electronic switch can operate at a very small interval of 0.1nsec between on and off. An adjustment circuit can control the detection timing from 0 to 4nsec by an interval of 0.1nsec. The analog circuit has a band width of 500KHz and AD (Analog Digital) converter has 16 bits. The I2C communication is used to send data to the MCU (Micro Controller Unit). Consumption current is about 0.4 mA @ ODR (Output Data Rate) of 5KHz.

The experiments using the GSR sensor produced through connecting with ASIC and GSR elements by wire bonding (Fig. 4(b)) are carried out to examine the effects of pulse frequency, detection timing, coil turn numbers and effective permeability on magnetic properties such as sensitivity, relationship between magnetic field and coil voltage, measuring range, linearity, noise and hysteresis. The effect of frequency is examined by changing the transition time of pulse current  $\Delta t$  from 0.2nsec to 1nsec where the pulse frequency  $f$  is defined by  $f = 1/2\Delta t$ .

### 3. Results on features of coil voltage of GSR sensor

The coil voltage of the GSR sensor [26,35] observed under a frequency of 1.5 GHz reaches the maximum value in about 1nsec and then decreases. The maximum value of coil voltage increases with the increase of the magnetic field and takes opposite values by positive and negative. It is noted that coil voltages at  $H = 0$  A/m meaning electric signal voltage is very small compared to that at  $H = 7200$  A/m, representing magnetic signal voltage. The relationship between the coil voltage and the magnetic field at the maximum detection timing of the falling process is shown in Fig. 5. There is a surprising result that this relationship is a sine function expressed in an equation as  $V = V_0 \sin(\pi H/2H_m)$  where  $H_m$  is defined as the field strength taking  $V_{max}$ . The experimental data results show that  $H_m$  is nearly equal to the anisotropy  $H_k$  of the amorphous wire, that is,  $H_m = 0.96H_k$ .

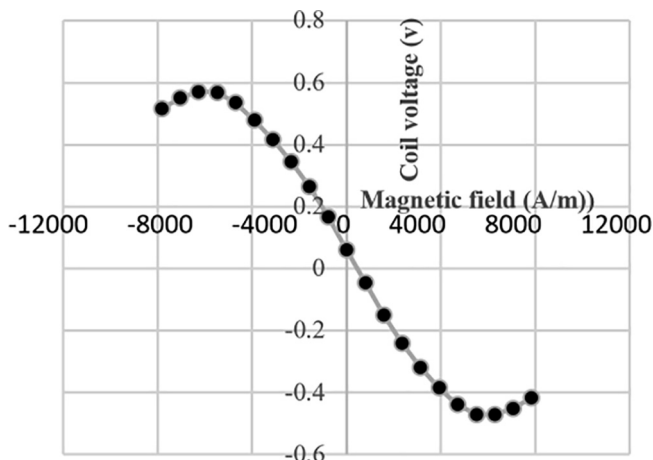


Fig. 5. Coil Voltage vs Magnetic Field.

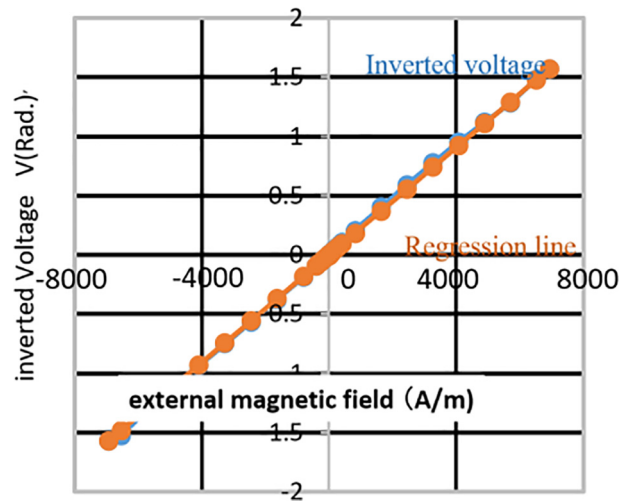


Fig. 6. Inverted Coil Voltage vs Regression Line.

Fig. 6 shows both linear lines of an inverted voltage by  $\pi H/2H_m = \arcsin(V/V_0)$  and a regression line. It is found that the linear relationship between coil voltage and magnetic field gives good linearity of 0.5% FS(= Full Scale) and an extension of the measuring range of 960 A/m (linear approximation) to 7200 A/m (dependent on  $H_m$ ). It is noted that when the frequency is under 0.5 GHz, the relationship does not show the sine functionality probably because it is influenced by the movement of 90 degree domain wall.

#### 3.1. Results on sensitivity of GSR sensor

The effect of pulse current frequency on the sensitivity of the GSR sensor type of length = 0.26 mm is studied by changing the frequency from 1 GHz to 3 GHz as shown in Fig. 7(a). The surprising result obtained is that the coil voltage increased with the increase of frequency following saturation of over 3 GHz. This result is caused by the high-speed spin rotation excited by the GHz pulse current. The spins existing in the surface would rotate at the angular velocity  $\omega (=2\pi f)$  and the phenomena must make the big coil voltage  $V(= -\Delta\phi/\Delta t)$  due to the high speed, without the movement of the 90 degree domain wall, existing between the surface domain with circular spin alignment and the core domain with the axis direction spin alignment.

It is well-known that the GMI effect is caused by skin effect of high frequency current accompanied by the movement of domain wall, and it reaches the maximum sensitivity at a frequency of 0.2 GHz. This is because the sensitivity of the GMI effect would decrease beyond 0.2 GHz due to the big eddy current caused by high frequency current.

The sensitivity tested under 1.5 GHz increases proportionally to the number of coil turns as shown in Fig. 7(b), where coil turn numbers change from 16 turns to 148 turns keeping their wire lengths of 0.96 mm. The increase of coil resistance and parasitic capacitance accomplished through increase of coil turn numbers are not affected under present test conditions.

It is found that the rising detection has two times larger sensitivity than the falling detection. The reason for this might be because the circular magnetic field induced by the rising pulse forces stronger magnetic torque to spins tilted by the external magnetic field. On the other hand, the falling pulse acts to decrease the circular magnetic field and spins would rotate to their own equilibrium state spontaneously with less magnetic torque.

#### 3.2. Results on other magnetic properties

Fig. 8 shows the result that  $\sigma$ -noise ( $\sigma =$  standard deviation) decreases to 40  $\mu V$  under  $H = 7200$  A/m when falling detection is carried

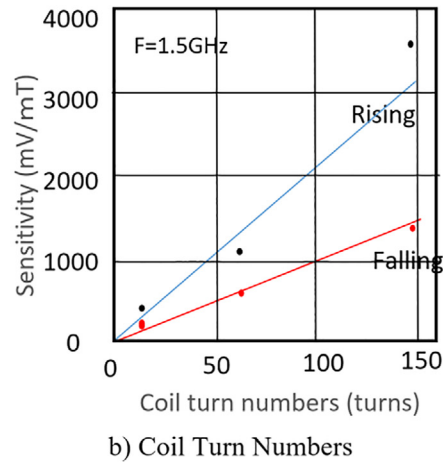
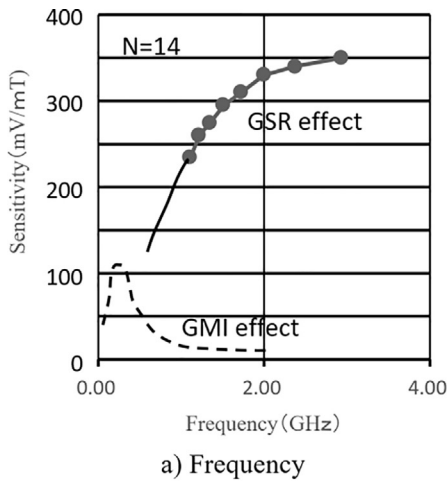


Fig. 7. Effect of Frequency and Coil Turn Numbers.

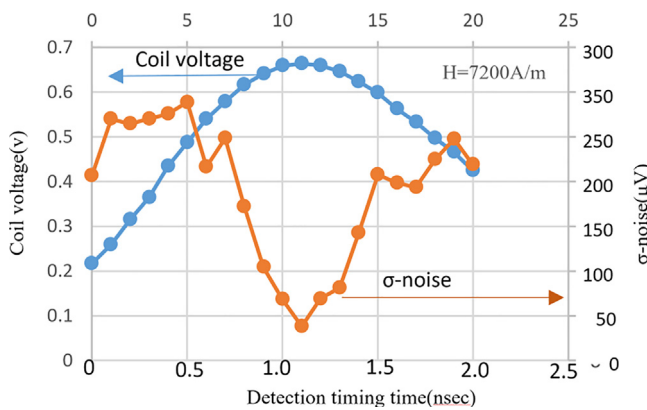


Fig. 8. Detection Timing vs  $\sigma$ -Noise.

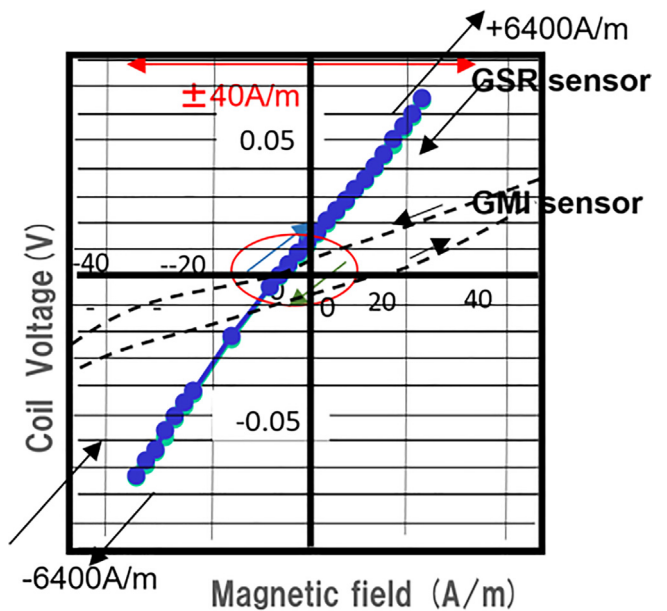


Fig. 9. Hysteresis of Rising detection.

out around the peak position of the coil voltage. This indicates that the magnetic noise of the GSR sensor is only 10  $\mu$ V, since ASIC has its own noise of 30  $\mu$ V. The frequency of pulse current takes the designated GHz frequency around peak position. High frequency generates spin rotation accompanied by low noise. But around the initial and ending time of pulse current it rises or falls slowly to take low frequencies of KHz to MHz. These low frequencies induce domain wall movement to make strong noise proportional to magnetic field strength.

As shown in Fig. 9, it is found that the rising detection of the GSR sensor, as well as falling detection, makes no hysteresis. The GSR effect only detects magnetization rotation brought by spin rotation around the wire surface therefore it is logical that hysteresis does not occur. On the contrary, the rising detection of GMI sensor shows a big hysteresis [36] expressed with the dotted line because it detects axial magnetization change to have the big hysteresis. Rising detection is important for developing high ODR type GSR sensor of over 1 MHz. This means that the GSR sensor has a greater potential ability than the GMI sensor.

Fig. 10(a) shows effects of the hysteresis of the B curve of the amorphous wire. The hysteresis increases by the tension annealing with the temperature of 400°C and tension of 20 kg/mm<sup>2</sup>, but the hysteresis does not appear in the GSR result in spite of the big BH curve hysteresis of the amorphous wire in Fig. 10(b). The reason is probably because the GSR effect is dependent only on the spin alignment in the surface but not related to the movement of the domain wall which makes hysteresis of the wire core.

### 3.3. Summary of the results

We observed the GSR effect based on the magnetization rotation

brought by the spin rotation of electron spins existing in the surface circular magnetic domain driven by GHz pulse current. The effect makes new features like enhanced sensitivity due to increase of coil voltage with pulse frequency of up to 2 GHz, its relationship with magnetic field and coil voltage has the sin functionality to extend the range of linearity, as well as it gives non hysteresis and low noise. These features are explained by spin rotation not accompanied by magnetic wall movements.

#### 3.3.1. Development of 3 dimensional photography process for a micro coil

We developed 3-dimensional photography process to produce a micro coil and to form it on the ASIC surface directly. The element is produced through the following process shown in Fig. 11 where a glass coated amorphous wire with a diameter of 10  $\mu$ m has a composition of Co<sub>50.7</sub>Fe<sub>8.1</sub>B<sub>13.3</sub>Si<sub>10.3</sub> and relative permeability of 1800.

The first step is to make a groove with a width of 18  $\mu$ m and a depth of 7  $\mu$ m on the film by RIE (Reactive Ion Etching) etching on the Si substrate. The second step is to produce a bottom coil pattern with a coil pitch of 5.5  $\mu$ m. The 3-dimensional photolithography makes wire pattern on the convex-concave plane controlled by diffraction phenomenon between mask lattice and convex-concave plane. The coil

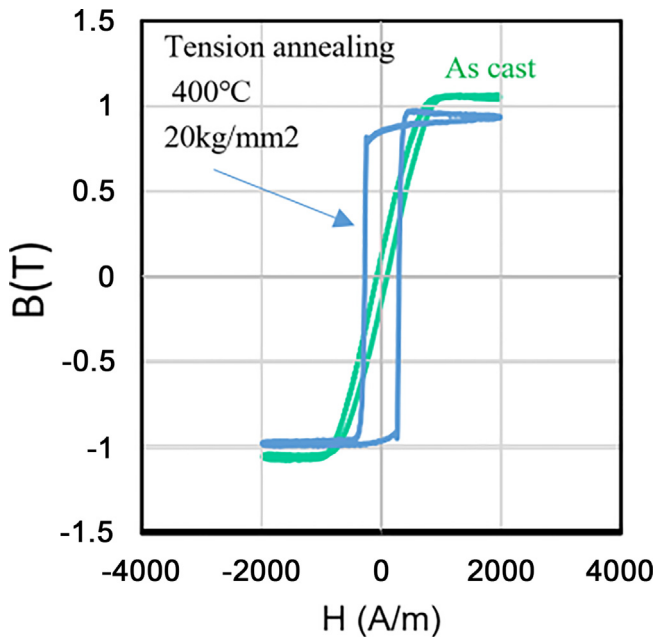


Fig. 10. BH curve of amorphous wire Hysteresis of Rising detection For Tension annealing at 400°C under 20 kg/mm<sup>2</sup>.

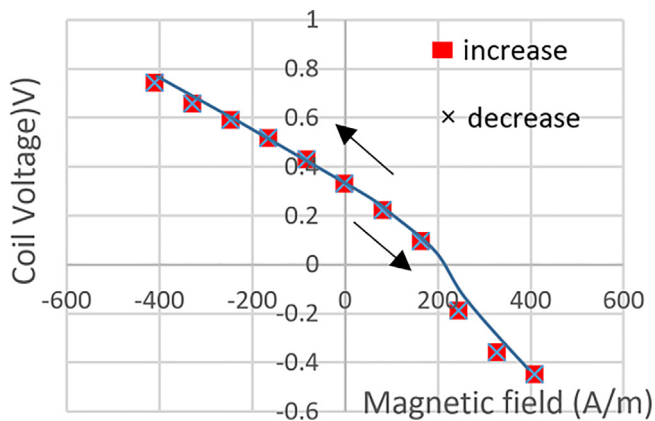


Fig. 10. (continued)

pitch of 5.5 μm can be formed by the combination with mask lattice pitch of 5.5 μm and groove depth of 7 μm using the light wavelength of 700 nm. The third step is to set the amorphous wire along the groove using a wire alimant machine. This machine can apply the tension of 76 kg/mm<sup>2</sup> to the wire with a diameter of 10 μm to improve linearity of the GSR sensor and can align wires with the alimant interval with ± 1 μm accuracy. The fourth step is to mold the wire by heating an adhesive resist at 280 °C and the fifth step is to produce a wire coil pattern with a coil pitch of 5.5 μm using 3-dimensional photolithography on the adhesive resist. Moreover, the electrical contacts are

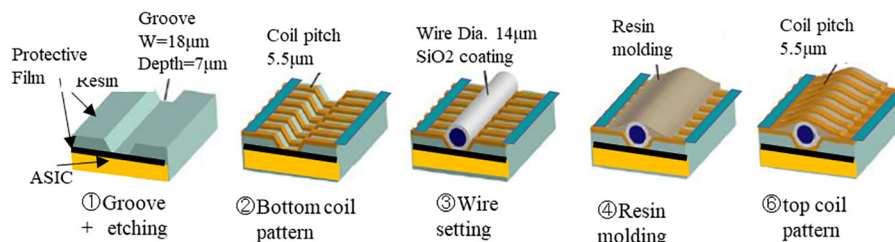


Fig. 11. Production Process to Produce GSR.

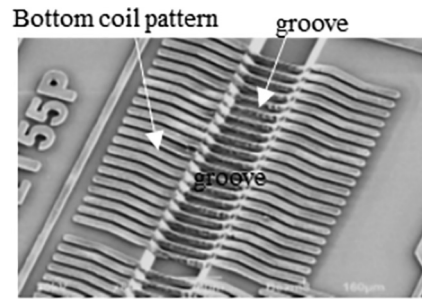


Fig. 12. Bottom Coil Pattern on the Groove.

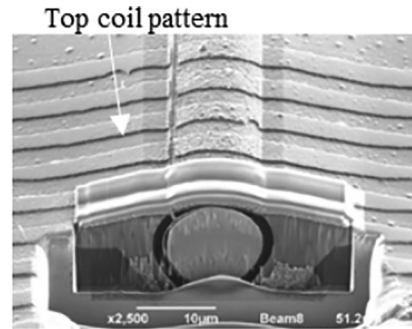


Fig. 13. Top Coil Pattern on the Convex.

produced on both ends of the glass-coated microwire by means of making metal contact between the wire and the electrodes after removal of the glass.

Fig. 12 and Fig. 13 show SEM(Scanning Electron Microscope) photos on Bottom Coil pattern on the groove and Top coil pattern on the convex respectively.

The above process can produce a micro coil with a coil pitch of 5.5 μm, coil diameter of 16 μm, wire length of 0.10 mm to 2 mm and number of coil turns from 10 turn to 148 turns on the ASIC surface directly shown in Fig. 14. The micro coil on-ASIC type GSR sensor which is formed on the ASIC surface can be drastically downsized as shown in Fig. 14. Moreover it has two-times larger sensitivity compared to the wire-bonding type GSR sensor in Fig. 15. The decrease is due to energy loss by bonding wires.

### 3.3.2. Development of ASIC type GSR sensor for various applications

Various prototypes of GSR Elements produced are shown in Fig. 16. They are divided into one axis type with the length of 0.16 mm, 0.45 mm and 0.99 mm, two axis type and three axis type.

Some prototype GSR sensors suitable for specified applications are produced by combining these elements and the ASIC. The properties of these prototype GSR sensors are shown in Table 1. It is noted that the examinations have been carried out using one ASIC, which means that their circuit performances are not optimized for all elements. Here it is suggested that the GSR sensor has good potential for some specified applications.

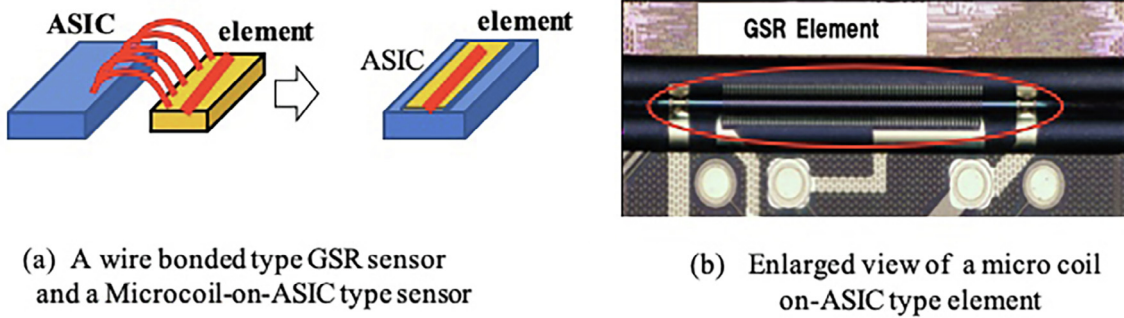


Fig. 14. Enlarged view of on-ASIC type element.

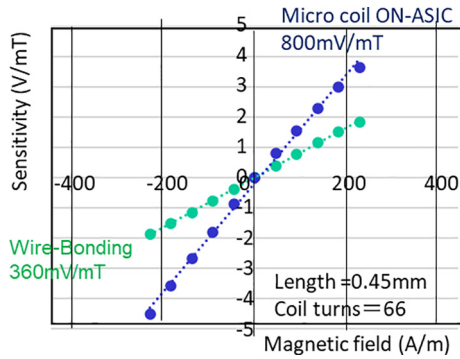


Fig. 15. Effect of assembling method to the sensitivity.

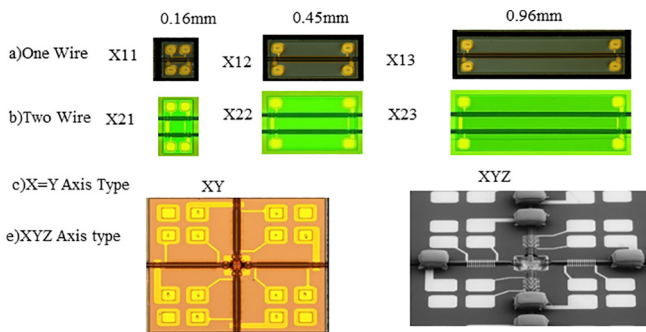


Fig. 16. Various Prototype GSR Element.

3.4. Automotive use application or robot industries

These applications request high accuracy and precise magnetic sensors of 16 to 18 bits with a wide measuring range of over 80G as well as high sensitivity, good linearity, no hysteresis, low noise, low consumption, and wide bandwidth of over 500KHz. Micro-coil-on-ASIC Type GSR Sensor such as Types of X11 and ASIC type GSR sensor as type of Types of X11 and X21 with wire length of 0.16 mm can achieve wide measuring range of over 6400 A/m, good linearity of 0.1%FS, almost no hysteresis, low  $\sigma$ -noise of 200nT to 600nT, low current consumption of 0.4 mA, 240nT/LSB in condition of analog circuit bandwidth of 500KHz and ODR of 5KHz. In addition, it is well known that the amorphous wire type sensors equip strong reliability and temperature stability against outside environmental factors such as temperature, magnetic damage, and mechanical stress.

GMI sensors have not been used in the automotive industry because of its narrow measuring range of 960 A/m. The prototype of the GSR sensor has a wide measuring range of over 6400 A/m as well as high total performance 100 times better than that of commercial ASIC type GMI sensor. Here the total performance is calculated by the performance index of S/N ratio  $\times$  measuring range  $\times$  element size.

3.5. Small size GSR sensor for in the body use

Micro-coil-on-ASIC Type GSR Sensor can make very small size possible because the GSR element can be produced directly on the ASIC surface. The GSR sensor can be made the same size as the ASIC with dimensions of 1.2 mm  $\times$  1.2 mm  $\times$  0.1 mm which is used in this paper. This means that the GSR sensor is promising for in body navigation use. The magnetic devices with  $\sigma$ -noise of over 1000nT for in body navigation such as catheters, endoscope and so on are used, but they have a poor positioning accuracy of 1 to 2 mm.

If types of X12 and X13 with the length of 0.45 mm and 0.90 mm

Table 1

Performance of various ASIC type GSR sensors.

Types	Element Size Length(mm) $\times$ Width (mm)	Resistance Wire/Coil $\Omega$	Coil Turn Numbers turn	Sensitivity mV/mT	$\sigma$ Noise @5KHz $\mu$ V nT	S/N Ratio	Measuring Range A/m	Typical Applications Futures
X11	0.16 $\times$ 0.23	Mar-80	14	100	60 600	167	6400	Automotive
X12	0.45 $\times$ 0.23	7/330	64	630	60 100	1050	2400	Wide range Positioning
X13	0.90 $\times$ 0.23	14/740	148	1400	140 100	1000	Over 800	sensitivity nT meter High sensitivity
X21	0.22 $\times$ 0.34	6/140	28	130	35 270	370	6400	Automotive
XY	0.26 $\times$ 0.3 XY:0.6 $\times$ 0.6	6/160	32	300	70 200 - 140	430	4000	Wide range Encoder
XYZ	0.26 $\times$ 0.3 XYZ:0.6 $\times$ 0.6	Jun-80	14	160	60 380 - 270	270	4000	2D Gyro Compass
*MI	0.60 $\times$ 0.35	10-Jan	16	33	70 7	47	960	3D compass compass

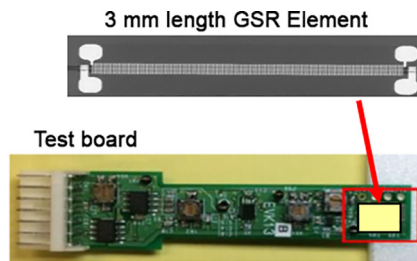


Fig. 17. nT sensor with 3 mm length element.

respectively with  $\sigma$ -noise of 100nT @ ODR of 5KHz is used, it is expected that the positioning accuracy will improve to under 0.1 mm. These applications request long and thin shaped sensors which make on-chip type GSR sensors an ideal choice, since a long magnetic wire is used in GSR sensors.

### 3.6. Compass for smart phone and mobile computer

Types of XY and XYZ are operated to output five data such X1, X2, Y1, Y2 and temperature @ODR of 1KHz. Type XY for 2D compass consists of two X-axis coil (X1 and X2) and two Y-axis coil (Y1 and Y2) to obtain the magnetic field at the center position by averaging to have noise of 140 nT @ ODR of 1KHz and range of 4000 A/m. Type XYZ for 3D compass consists of 2D compass and permalloy parts to detect the Z-axis magnetic field. The sensitivity for the Z-axis magnetic field is adjusted by the height of the permalloy part. It is important to form a magnetic circuit by direct connection with the wire and the permalloy parts. It has noise of 270nT @ ODR of 1KHz and the range of 4000 A/m.

Types of XY and XYZ are designed to be suitable for next generation compasses that request noise of under 100nT @ODR of 200 Hz and measuring range of 1920 A/m, compared to current specification of noise of under 1000nT @ ODR of 50 Hz and the range of 960 A/m. The new specification is about 20 times higher than the conventional one. Types of XY and XYZ have not yet satisfied the specification, but if the ASIC performance or the GSR element design are changed to make ODR from 1KHz to 200 Hz and measuring range from 4000 A/m to 1920 A/m,  $\sigma$ -noise will decrease from 140nT to about 30nT to satisfy the specifications for the next generation compasses. The next generation compasses will have high speed and accuracy so that it can calculate real time 3-dimensional attitude. That is, the next generation compasses will be a magnetic Gyro-Compass with gyro functionality without the vibration type gyro sensor. This type of GSR sensor must be promising for uses in smartphones, mobile computers, drones, robots, and VR (Virtual Reality) /AR(Augmented Reality) headsets.

### 3.7. pT sensor for detecting biomagnetism

The sensitivity of the GSR sensor in Fig. 17 can increase to 15000 mV/mT by extending the long wire or having four short wires for the GSR element, which would increase the number of coil turns from 500 to 1000 turns. GSR sensor with  $\sigma$ -noise of 0.4nT will be promising for these applications. However the wire resistance of the long coil would become more than 2K $\Omega$ , which means that we need to make a high power electronic circuit with Voltage Domains) of 5 V.

## 4. Summary

We observed a new phenomenon where the GHz pulse increases the coil voltage winded around the amorphous microwire and the relationship with the coil voltage and magnetic field shows sine functionality. We assumed that this new phenomenon was caused by the magnetization rotation brought by spin rotation in the surface domain with circularly oriented alignment and named it the GSR effect.

Based on the GSR effect, we developed the GSR sensor which provides new features with enhanced sensitivity and sine functional relationship with magnetic field as well as good linearity, non-hysteresis and low noise.

We developed the production technology to form micro coils directly on the ASIC surface, and with this technology we can create smaller sized GSR sensor, or micro-coil-on-ASIC Type GSR Sensor. This micro-coil-on-ASIC type has 2 times better sensitivity than that of ASIC type wire bonded with GSR element and ASIC.

Sensitive and fast-response micro-sensors are recently evaluated as the leading technology for innovative measurement and control system in creation of new industries. The GSR sensor has all the chances to dominate the magnetic sensor industry, both for its revolutionary technology and attractive cost performance. The GSR sensor features high sensitivity, fast response, and low energy consumption, all while staying micro sized, which make them unique when compared to other magnetic sensors like magneto-resistance sensors (AMR, GMR, TMR), Hall sensors and induction sensors.

Some prototypes of ASIC type GSR sensor have been produced in consideration for applications in automotive use, in body use, gyro-compass use and medical use. It is concluded that GSR sensors have the potential to become a promising magnetic sensor for many applications in the future.

### CRediT authorship contribution statement

**Yoshinobu Honkura**: . : Conceptualization, Methodology, Formal analysis, Resources, Data curation, Writing - original draft, Visualization, Supervision, Project administration. **Shinpei Honkura**: Validation, Investigation.

### Declaration of Competing Interest

The authors declare that they have no known competing financial interests or personal relationships that could have appeared to influence the work reported in this paper.

### Acknowledgment

This work was financially supported by the subsidized projects of METI, NEDO and Aichi Prefecture of Japan. We wish to acknowledge these supports.

### Appendix A. Supplementary data

Supplementary data to this article can be found online at <https://doi.org/10.1016/j.jmmm.2020.167240>.

### References

- [1] J. Lenz, A.S. Edelstein, *IEEE Sens. J.* 6 (3) (2006) 631–649.
- [2] M. Díaz-Michelena, Small magnetic sensors for space applications, *Sensors* 9 (2009) 2271–2283.
- [3] P. Ripka, G. VeHrtesy, *Sensors based on soft magnetic materials Panel discussion*, *J. Magn. Magn. Mater.* 215–216 (2000) 795–799.
- [4] Y. Honkura, The development of Magnetic sensors and their highlight markets, *Magnetics Jpn.* Vpl. 3. No.11.p538-545 (2008).
- [5] T. Masumoto, I. Ohnaka, A. Inoue, M. Kawamura, *Scr. Metal.*, 15 (1981) p293.
- [6] H. Hagiwara, A. Inoue, T. Masumoto, *MetalTrans* A13 (1982) p373.
- [7] F.B. Humpgrey, A. Inoue, T. Masumoto et al., *Elsevier Amsterdam*, (1987) p110.
- [8] J. Yamzaki, F.B. Humpgrey, K. Mohri, H. Kawamura, H. Takemura, R. Malmhall, *J. Mag. Soc. Jpn.* 12 (1985) p245.
- [9] Y. Akane, *Magnetic Sensors*, Japan Patent No.2617498(1987).
- [10] V.E. Makhotkin, B.P. Shurukhin, V.A. Lopatin, P.Y. Marchukov, Y.K. Levin, *Magnetic field sensors based on amorphous ribbons*, *Sens. Actuators, A* 27 (1-3) (1991) 759–762.
- [11] K. Mohri, K. Kawashima, T. Kohzawa, H. Yoshida: *IEEE Trans.Magn.*, V29, p1245-1248(1993).
- [12] L.V. Panina, K. Mohri, *Magneto-impedance effect in amorphous wires*, *Appl. Phys. Lett.* 65 (1994) 1189–1191.

- [13] K. Mohri supervisor; [Science and technology on magnetic sensors], Corona Publishing Co. LTD (1998).
- [14] D. Ménard, M. Britel, P. Ciureanu, A. Yelon, Giant magnetoimpedance in a cylindrical conductor, *J. Appl. Phys.* 84 (1998) 2805–2814.
- [15] L.V. Panina, D.P. Markhnovskiy, K. Mohri, Magnetoimpedance in amorphous wires and multifunctional applications, *J. Magn. Magn. Mater.* 272-276 (2004) 1452-1459 GMI 2GHz.
- [16] Y. Kabanov et al., Magnetic domain structure of microwires studied by using the magneto-optical indicator film method, *Appl. Phys. Lett.* 87. P142507(2005).
- [17] A. Zhukov, V. Zhukova, J.M. Blanco, J. Gonzalez, Recent research on magnetic properties of glass-coated microwires, *J. Magn. Magn. Mater.* 294 (2005) 182–192.
- [18] K. Mohri, A micro magnetic sensor based on MI effect, Japan Patent No. 3645116 (1999).
- [19] Y. Honkura, Development of amorphous wire type MI sensors for automobile use, *J. Magn. Magn. Mater.* 249 (2002) 375–381.
- [20] Mohri supervisor, New magnetic sensors and their applications, Triceps Co. Ltd, (2013).
- [21] S. Sandacci, D. Makhnovkiy, L. Pania, K. Mohri, Y. Honkura, Off-diagonal impedance in amorphous wires and its application to linear magnetic sensors, *IEEE Trans. Magn.* V40 (6) (2004) p3505.
- [22] Y. Honkura, The development of MI sensor and its applications, AMMTA p71-94(2008) ISBN:978-81-7895-367-0.
- [23] Y. Honkura, chapter3: Electronics compass and motion sensor using MI sensor, [new magnetic sensors and their applications] Triceps Co. Ltd, (2013).
- [24] T. Uchiyama, K. Mohri, Sh. Nakayama, Measurement of spontaneous oscillatory magnetic field of guinea-pig smooth muscle preparation using pico-tesla resolution amorphous wire magneto-impedance sensor, *IEEE Trans. Magn.* 47 (2011) 3070–3073.
- [25] A. Zhukov, A. Talaat, M. Ipatov, V. Zhukova, High Frequency Giant Magnetoimpedance Effect of amorphous microwires for magnetic sensors applications, Proceeding of 8th International Congress on Sensing Technology, Sep.2-4 (2014) p524.
- [26] Y. Honkura, Update on development of extremely high sensitive micro magnetic sensor “GSR sensor” Text book of 4th study group meeting of MSJ on extremely high sensitive micro magnetic sensors, No.4, p10-15(2016).
- [27] S. Gudoshnikov, N. Usov, A. Nozdrin, M. Ipatov, A. Zhukov, V. Zhukova, Highly sensitive magnetometer based on the off-diagonal GMI effect in Co-rich glass-coated microwire, *Phys. Stat. Sol. (a)* 211 (5) (2014) 980–985.
- [28] A. Zhukov, A. Talaat, M. Ipatov, V. Zhukova, Tailoring of high frequency giant magnetoimpedance effect of amorphous co-rich microwires, *IEEE Magn. Lett.* 6 (2015) 2500104.
- [29] A. Zhukov et al., Trends in optimization of Giant Magnetoimpedance effect in amorphous and nanocrystalline materials, *A. Alloys Compound.* 727(2017) 887-901.
- [30] V. Zhukova, J.M. Blanco, M. Ipatov, J. Gonzalez, M. Churyukanova, A. Zhukov, Engineering of magnetic softness and giant magnetoimpedance effect in Fe-rich microwires by stress-annealing, *Scr. Mater.* 142 (2018) 10–14, <https://doi.org/10.1016/j.scriptamat.2017.08.014>.
- [31] V. Zhukova, M. Ipatov, A. Talaat, J.M. Blanco, M. Churyukanova, S. Taskaev, A. Zhukov, Effect of stress-induced anisotropy on high frequency magnetoimpedance effect of Fe and Co-rich glass-coated microwires, *J. Alloys Compound.* 735 (2018) 1818–1825.
- [32] Y. Uehara et al., Analysis on the dynamic magnetic process of amorphous wire using LLG equation” Text book of 1th study group meeting of MSJ on extremely high sensitive micro magnetic sensors, No.1, p15-21(2015).
- [33] Y. Honkura, chapter 5 section4: Development of high sensitive micro magnetic sensor based on GSR effect, [new magnetic sensors and their applications] Technical Information Institute Co. LTD (2018).
- [34] Y. Honkura, High Sensitive Micro sized Magnetometer, United States Patent No: US 9,857,436 B2, Jan. 2, 2018.
- [35] Y. Honkura, S. Honkura, The development of ASIC type GSR sensor driven by GHz pulse current, *SensorDevices* p15-21 (2018), ISBN:978-1-61208-610-6.
- [36] Y. Honkura, S. Honkura, The development of a High sensitive micro size magnetic sensor named as GSR sensor excited by Ghz pulse current, ASIC type GSR sensor driven by GHz pulse current” *PIERS* p324-331 (2018).